CF_3CFHO versus CH_3CH_2O: An ab Initio Molecular Orbital Study of Mechanisms of Decomposition and Reaction with O_2

Jonathan E. Stevens,* Reem A. Jabo Khayat, Olga Radkevich, and Jessica Brown

Department of Chemistry and Biochemistry, University of Detroit Mercy, Detroit, Michigan 48219

Received: July 15, 2004; In Final Form: October 6, 2004

Ab initio electronic structure calculations provide potential energy surfaces for the decomposition of CF_3CFHO and its competing reaction with O_2. Additional calculations with the same methods study the analogous reactions of the unfluorinated analogue CH_3CH_2O. We use transition state theory, incorporating data from the ab initio computations, to model rate constants for all of these reactions. Comparisons are made between fluorinated and unfluorinated systems as well as to experiment.

I. Introduction

Hydrofluorocarbon 134a (CF_3CFH_2) is a chlorofluorocarbon replacement used in air conditioning systems and refrigerators. It has been established that it has no impact on stratospheric ozone.[1] However, CF_3CFH_2 released into the atmosphere may be oxidized through a sequence of reactions to produce the CF_3CFHO radical.[2,3] This radical may then undergo two possible atmospheric reactions:

$$CF_3CFHO + O_2 \rightarrow CF_3COF + HOO \tag{1}$$

$$CF_3CFHO \rightarrow CF_3 + FCHO \tag{2}$$

The branching between these two reactions is competitive, both of these reactions have been the subject of recent experimental[2−8] study, and reaction 2 has been the recent subject of several computational[8−10] studies. Reaction 2 is a thermal decomposition reaction subject to collisional activation. Reaction 1 is of particular interest as it produces CF_3COF, which may be hydrolyzed to CF_3COOH in the atmosphere and precipitated in rainwater. It has been suggested that CF_3COOH precipitation may have an ecological impact on wetlands over time.[11]

Experiments[2−8] on these two reactions determine the rate constant ratio k_1/k_2. This quantity varies due to the pressure dependence of reaction 2,[5−7] but at 1 atm pressure the ratio is well described[7] by the Arrhenius expression

$$k_1/k_2 = 2.4 \times 10^{-25} \exp[3590(\pm 150))/T] \text{ cm}^3$$

which gives a ratio of 4.0×10^{-20} cm^3 at 298 K and 1 atm.

It is natural to consider the relationship between the rates of reactions 1 and 2 with the rates of reaction of the unfluorinated alkoxy radicals. Recent research has given rise to two questions on this topic. The first concerns the relative rate of reaction 1 to the rate of reaction of unfluorinated alkoxy radicals with O_2. Bednarek et al.[5] use experimental data and simulations to obtain a somewhat uncertain value of $k_1 = 2.7 \times 10^{-15}$ cm^3/molecule*s at 296 K and 38 Torr; while uncertain, this matches a value previously obtained by Zellner, as reported in ref 2.[12] A recent computational study of reaction 2 by Somnitz and Zellner[10] reports a recent estimate of 4.2×10^{-16} cm^3/s for the value of k_1, obtained from a value of k_2 determined by ab initio/RRKM modeling and the Arrhenius expression for k_1/k_2 noted previously. Wu and Carr[8] also combine ab initio/RRKM modeling of reaction 2 with experimental results to obtain possible k_1 values of 4.75×10^{-15} and 1.9×10^{-14} cm^3/s at 295 K. Wu and Carr also studied the reaction of $CFCl_2CH_2O$[13] and obtained a rate constant of 1.0×10^{-16} cm^3/s at 298 K. Wallington[6] compares the experimental rate constants reported by Bednarek et al.[5] and Wu and Carr[13] to the rate constant for the reaction of CH_3CH_2O with O_2, which at 298 K is 1.0×10^{-14} cm^3/s,[14,15] and speculate that the rate constants for the reaction of fluorinated ethoxy radicals with O_2 are 1−2 orders of magnitude smaller than their unfluorinated analogues, a conclusion shared by Somnitz and Zellner.[10]

An additional question concerns the Arrhenius *A* factors of reactions 1 and 2 in comparison to their unhalogenated analogues. Schneider et al.[9] observe that, according to Benson,[16] *A* factors for C−C breaking in unhalogenated alkoxy radicals are typically in the range 3×10^{12} to 10^{14} s^{-1}. *A* factors for reaction with O_2 are taken as approximately equal to $2n_H \times 10^{-14}$ cm^3/s, where n_H is the number of hydrogens bonded to the carbon adjacent to alkoxy oxygen.[17] Schneider et al.[9] argue that if CF_3CFHO behaved in a manner consistent with its unfluorinated analogues, the ratio of *A* factors A_1/A_2 would be expected to have an approximate value between $[(2.0 \times 10^{-14})/(3.0 \times 10^{12})]$ and $[(2.0 \times 10^{-14})/(1.0 \times 10^{14})]$, or between 7×10^{-27} and 2×10^{-28} cm^3, numbers 2−3 orders of magnitude smaller than Wallington's value[7] of 2.1×10^{-25} cm^3 for the *A* factor ratio.

Schneider et al.[9] calculated the Arrhenius parameters of reaction 2 using intensive ab initio calculations and canonical transition state theory. They found an *A* factor comparable to that of nonhalogenated alkoxy radicals and concluded that reaction 1 must have an *A* factor much higher than what is expected when compared to nonhalogenated radicals.

The alkoxy radical reactions analogous to 1 and 2 are the reactions of the ethoxy radical, CH_3CH_2O:

$$CH_3CH_2O + O_2 \rightarrow CH_3CHO + HOO \tag{3}$$

$$CH_3CH_2O \rightarrow CH_3 + CH_2O \tag{4}$$

Several experimental studies have examined the rates of (3)[14,18,19] and (4),[20−23] and reaction 4 has been a subject of study

---

* Corresponding author. E-mail: stevenje@udmercy.edu.

10.1021/jp0468509 CCC: $27.50 © 2004 American Chemical Society
Published on Web 11/25/2004

by ab initio calculations.[22−25] The mechanism of reaction of CH_3CH_2O with O_2 has not been studied with computational methods, but some ab initio quantum computational studies of the reaction of CH_3O with O_2,

$$CH_3O + O_2 \rightarrow CH_2O + OOH \tag{5}$$

have been reported.[26,27] Initially, reaction with O_2 was predicted to proceed by formation of a trioxy intermediate, with OOH then formed by elimination:

$$CH_3O + O_2 \rightarrow CH_3OOO \tag{5a}$$

$$CH_3OOO \rightarrow CH_2O + OOH \tag{5b}$$

This mechanism was advanced to explain low *A* factors in the reaction of alkoxy radicals with O_2.[9,26] However, Bofill et al.[27] have recently studied the reaction of O_2 with CH_3O with exhaustive ab initio computations; their results indicate that the initial computational study[26] misidentified the reaction pathway and that OOH is likely to be formed via a direct abstraction process.

In summary, existing research engenders the following three questions: (1) Does CF_3CFHO in particular, or fluorinated radicals in general, react more rapidly with O_2 than unfluorinated ones? (2) If so, is this the result of marked differences in the mechanism of reaction of fluorinated and unfluorinated radicals with O_2? (3) Is the *A* factor for the reaction of CF_3CFHO with O_2 abnormally large, as suggested by Schneider et al.,[9] or is there another explanation for the large *A* factor ratio A_1/A_2? As noted above, reactions 1 and 4 have not yet been studied with quantum computational approaches. To elucidate the questions outlined above, this work presents ab initio molecular orbital investigations and subsequent modeling of rate constants for reactions 1−4. The reactions are studied by consistent electronic structure and kinetic modeling approaches to facilitate comparisons of barrier heights to reactions and parameters arising from kinetic modeling. The method of our ab initio calculations is outlined in section II. Section III describes the resulting reaction potential energy surfaces, section IV discusses our modeling of rate constants, and section V summarizes the results.

II. Computational Methods

All calculations were completed using the Gaussian 98 electronic structure package.[28] Unless otherwise noted, all minima and transition states were optimized on a single doublet potential energy surface using the B3LYP hybrid density functional method.[29] A 6-311G(d,p) basis set, referred to as basis set I, was used for all atoms. Reactants and products were also optimized with the B3LYP/I method, with the appropriate ground-state spin multiplicity (singlet for closed-shell species, doublet for all species with an odd number of electrons, and triplet for O_2). B3LYP/I frequency calculations were performed for all optimized species. These frequency calculations verify that all frequencies for minima are real and that all transition states have one imaginary frequency. In the case of all optimized transition states, intrinsic reaction coordinate (IRC) calculations have established connectivity to reactants and products.

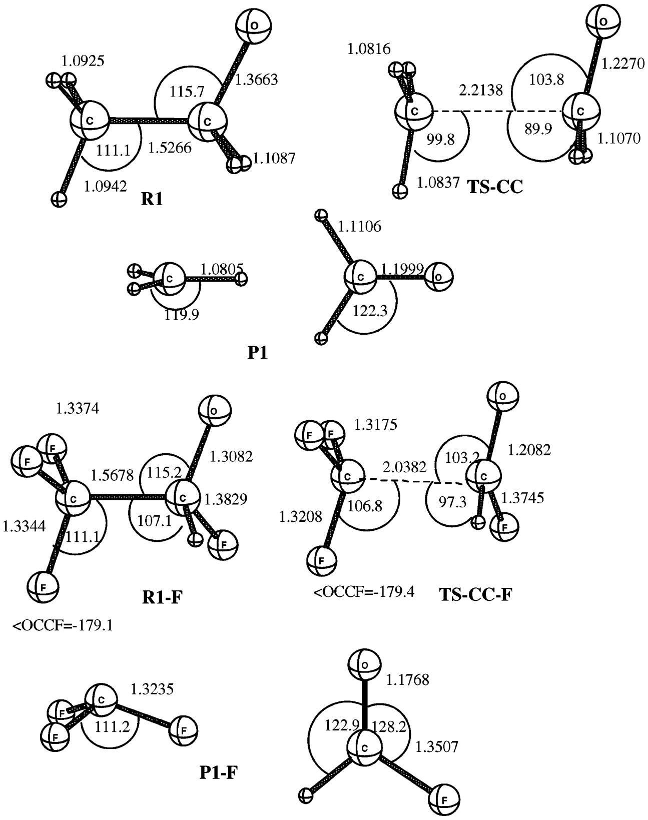

Figure 1. Structures of reactants, transition states, and products for the decomposition reactions of CH_3CH_2O and CF_3CFHO, as optimized with B3LYP/I computations. All bond lengths are in angstroms and angles are in degrees.

The G2M(CC,MP2) method[30] was used to calculate higher-level energies for all geometries optimized with the B3LYP calculations described above. This method of calculating single-point energies involves a CCSD(T)/I calculation to determine a base energy. A pair of MP2 calculations to establish a basis set correction follows this calculation. One MP2 computation determines the energy with a large 6-311+G(3df,2p) basis. This basis set is referred to as basis set II. The basis set correction is found by subtracting the calculated energy of an MP2/I calculation from the energy of a MP2/II calculation and then adding this difference to the CCSD(T)/I base energy. An additional zero-point energy (ZPE) correction determined at the B3LYP/I level is added to the base energy, as well as an empirical high-level correction (HLC) determined by the number of α and β electrons. The HLC energy is defined as $E[\mathrm{HLC}] = -5.30n_\beta - 0.19n_\alpha$, in units of millihartree, where n_β is the number of β electrons and n_α is the number of α electrons. The G2M(CC,MP2) energy is thus computed as

$$E[\mathrm{G2M(CC,MP2)}] = E[\mathrm{CCSD(T)/I}] + E[\mathrm{MP2/II}] - E[\mathrm{MP2/I}] + E[\mathrm{ZPE(B3LYP/I)}] + E[\mathrm{HLC}]$$

Some additional intensive calculations have been made using the CCSD(T) method with a cc-PVTZ basis set. This basis set will be referred to as basis set III.

III. Results

In the following sections, energies of optimized structures are reported relative to reactants for reactions 1−4, as appropriate. B3LYP/I, B3LYP/I + ZPE, and G2M(CC,MP2) energies are reported. B3LYP/I results will appear first in the text, followed in parentheses by B3LYP/I+ZPE in italic and G2M(CC,MP2) results in bold.

A. Potential Energy Surfaces for C−C Bond Breaking. Figure 1 shows the optimized transition state for C−C bond breaking, **TS-CC**, in the unfluorinated ethoxy radical, and its analogue for the CF_3CFHO reaction, **TS-CC-F**. The reactants, CH_3CH_2O (**R1**) and CF_3CFHO (**R1-F**), and products CH_3 and CH_2O (**P1**) and CF_3 and CFHO (**P1-F**) are also displayed.

For both the fluorinated and the unfluorinated radical, the transition state for C−C breaking is rather late. **TS-CC** appears at an energy of 19.8 (*17.8*, **16.4**) kcal/mol; the energy of reaction is 16.9 (*11.9*, **8.6**) kcal/mol. The corresponding enthalpies of reaction at 298 K (using thermal correction at 298 K as determined by B3LYP frequency calculation) are 13.1 (**10.1**) kcal/mol.

Early experimental determinations[20,21] of the activation energy for this reaction obtain a value of 21.6 kcal/mol. As noted in section III-C, the experimental enthalpy of reaction is 12.8 kcal/mol, and G2M(CC,MP2) computations underestimate this enthalpy by approximately 3 kcal/mol. Several ab initio studies have been made of this reaction. The PMP4/6-31G* calculations of Gonzales et al.[25] find a barrier of 22 kcal/mol for C−C breaking and an energy of reaction of 18.6 kcal/mol. Hoyermann et al.[23] determine a barrier of 20.8 kcal/mol for C−C breaking with MP2 methods. Somnitz and Zellner find barriers of 18−19 kcal/mol with a variety of model chemistries.[24] Caralp et al., in a study involving both computation and experiment,[22] implement BAC-MP4 computations and find a barrier of 17.4 kcal/mol and an enthalpy of reaction of 9.6 kcal/mol. The experimental results and most of the ab initio calculations noted here suggest that the G2M(CC,MP2) method underestimates both the barrier height and the endothermicity of this reaction, but the most recent results of Caralp et al.[22] are more in accord with the G2M(CC,MP2) calculations.

TS-CC-F appears at an energy of 9.7 (*8.7*, **11.3**) kcal/mol, and the energy of reaction is 1.76 (*0.18*, **1.46**) kcal/mol. These results are comparable to values obtained by the intensive ab initio calculations of Schneider et al.,[9] which find the barrier to C−C fission in CF_3CFHO to be 10.7 kcal/mol and the energy of reaction to be −0.3 kcal/mol. The rigorous G2 and G2(MP2) calculations of Wu and Carr[8] also find comparable values of 9.5 kcal/mol (G2 and G2(MP2)) for the barrier and values of 1.10 kcal/mol (G2) and 0.62 kcal/mol (G2(MP2)) for the energy of reaction. Somnitz and Zellner performed ab initio studies of this reaction and find a higher barrier of 12.6−13.1 kcal/mol with a variety of model chemistries.[10] Bednarek et al.[5] cite a value of −8.1 kcal/mol[31] for the enthalpy of reaction, in poorer agreement with our results; this is discussed further in section III-C.

B. Potential Energy Surfaces for Direct H-Abstraction Reaction with O_2. Bofill et al.[27] studied the potential energy of the $CH_3O + O_2$ reaction with the B3LYP method as well as with CISD, CASSCF, and QCISD(T) methods, taking CCSD(T)/cc-pVTZ single-point energies at optimized structures. Figure 2 presents a reaction profile for the $CH_3O + O_2$ reaction as determined by these calculations. Bofill et al.'s computations found two low-energy transition states for H-abstraction, one at an energy of 11.6 kcal/mol relative to the reactants and another, more stable one with a C−H−O−O−O ringlike structure at a relative energy of 3.7 kcal/mol. IRC computations verified that these transition states connect to $CH_3O + O_2$ reactants and CH_2O + OOH products through weakly bound hydrogen-bonding intermediates. While these calculations were able to optimize stable trioxy intermediates, these intermediates did not lie on the low-energy reaction pathway. This mechanism for H-abstraction was consistently found using the B3LYP method for optimizations as well as more computationally demanding approaches.

A pathway for H-abstraction initiating from a trioxy intermediate could not be determined with B3LYP optimizations. CISD and CASSCF optimizations, however, could determine a reaction pathway initiating from a “trans” trioxy intermediate.

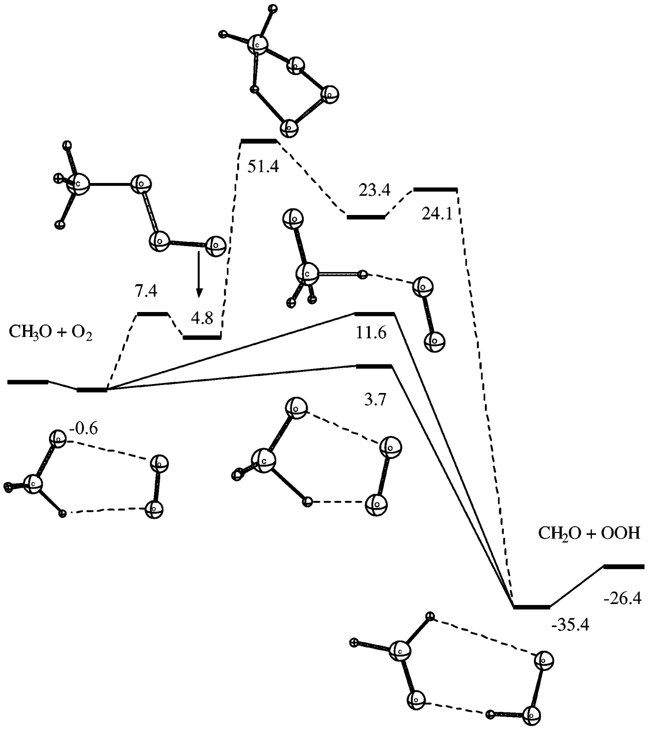

Figure 2. Computed CCSD(T)/cc-pVTZ//CASSCF/6-311G(d,p) reaction path for $CH_3O + O_2 \rightarrow CH_2O$ + OOH, as presented in ref 21. Energies are relative to reactants and are in kcal/mol.

The highest barrier on this reaction pathway appeared at an energy of 51.4 kcal/mol relative to the reactants, and Bofill et al.[27] concluded that the reaction would not occur by this route and that the favored H-abstraction pathways would be the low-energy, direct ones.

Our computations implement B3LYP/I optimizations to explore reaction pathways for the reactions of CH_3CH_2O and CF_3CFHO with O_2. For both alkoxy radicals, these calculations find two-direct abstraction transition states entirely analogous to the transition states of the $CH_3O + O_2$ reaction. For both radicals, these transition states lie on a reaction pathway which does not involve the formation of trioxy radical intermediates. Figure 3 shows optimized structures on the direct reaction pathway for the $CH_3CH_2O + O_2$ reaction. Figure 4 presents optimized structures on the direct reaction pathway for the $CF_3CFHO + O_2$ reaction. Figure 5 presents reaction profiles for both of these reactions, summarizing the energetics.

The CH_3CH_2O and O_2 reactants (**R2**) initially form a weakly bound complex **H-C1** in which O_2 interacts with hydrogen and oxygen atoms on the radical. The relative energy of **H-C1** is −0.9 (*0.01*, **10.4**) kcal/mol; the high G2M(CC,MP2) energy appears at the CCSD(T)/I, MP2/I and MP2/II levels of the G2M(CC,MP2) calculations. This complex connects directly to two transition states, **TS-A**, appearing at 8.9 (*7.5*, **10.4**) kcal/mol, and **TS-B**, a more stable transition state with a relative energy of 5.1 (*5.4*, **6.1**) kcal/mol. Both of these transition states connect **H-C1** to another complex, **H-C2**, with a relative energy of −40.2 (*−37.2*, **−45.2**) kcal/mol. This complex is connected to the CH_3CHO + OOH products (**P2**) without reverse barrier. The relative energy of **P2** is −28.4 (*−28.7*, **−36.9**) kcal/mol. For comparison, the experimental enthalpy of reaction is −32.7 kcal/mol, as discussed in section III-C.

For the $CF_3CFHO + O_2$ reaction, reactants (**R2-F**) may initially form one of two hydrogen-bonded intermediates, one in which an oxygen atom on O_2 interacts with an F atom on CF_3CFHO (**H-C1-A-F**) and another featuring an interaction

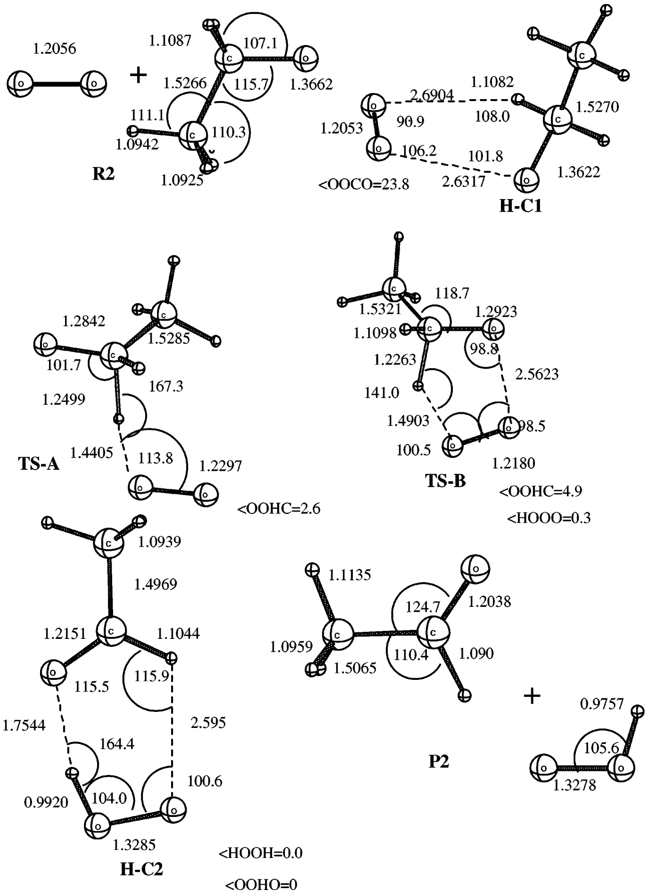

Figure 3. B3LYP/I structures of reactants, transition states, and products for the reaction of CH_3CH_2O with O_2. All bond lengths are in angstroms and angles are in degrees.

between an O_2 oxygen and an O atom on CF_3CFHO (**H-C1-B-F**). Both complexes are weakly bound; the relative energy of **H-C1-A-F** is −1.2 (*−0.8*, **−5.9**) kcal/mol, while the relative energy of **H-C1-B-F** is −1.4 (*−0.7*, **−4.3**) kcal/mol. **H-C1-A-F** connects to the transition state **TS-A-F**, the fluorinated analogue to **TS-A**, at a relative energy of 7.4 (*5.4*, **7.9**) kcal/mol. **H-C1-B-F** connects to the analogue of **TS-B**, **TS-B-F**, at a relative energy of 4.2 (*3.3*, **4.1**) kcal/mol. Both of these transition states connect to a hydrogen-bonded complex **H-C2-F** at a relative energy of −39.0 *(−36.6*, **−45.1**). This complex connects to the products CF_3COF and OOH (**P2-F**) without reverse barrier. The relative energy of **P2-F** is −31.8 (*−31.1*, **−39.3**) kcal/mol. For comparison, Bednarek et al.[5] cite a value of −38 kcal/mol[31] for the enthalpy of reaction, in good agreement with our results; this will be discussed further in section III-C.

C. Comparison to Experimental Enthalpies of Reaction. Comparison of computed enthalpies of reaction to experimental data provides some measure of the accuracy of the energetics reported in previous sections. Table 1 displays B3LYP/I, G2M(CC,MP2), and experimental enthalpies at 298 K for the reactions 1−4. The enthalpy of an optimized reactant or product is taken as the base energy (B3LYP/I or G2M(CC,MP2) with no ZPE correction) and the standard gas-phase enthalpy correction at 298 K as determined by Gaussian 98 B3LYP/I frequency computations and subsequent statistical mechanical evaluation.[32] The statistical mechanics calculation assumes an internally rigid molecule; that is, all of the internal degrees of freedom are treated as vibrations and not internal rotations.

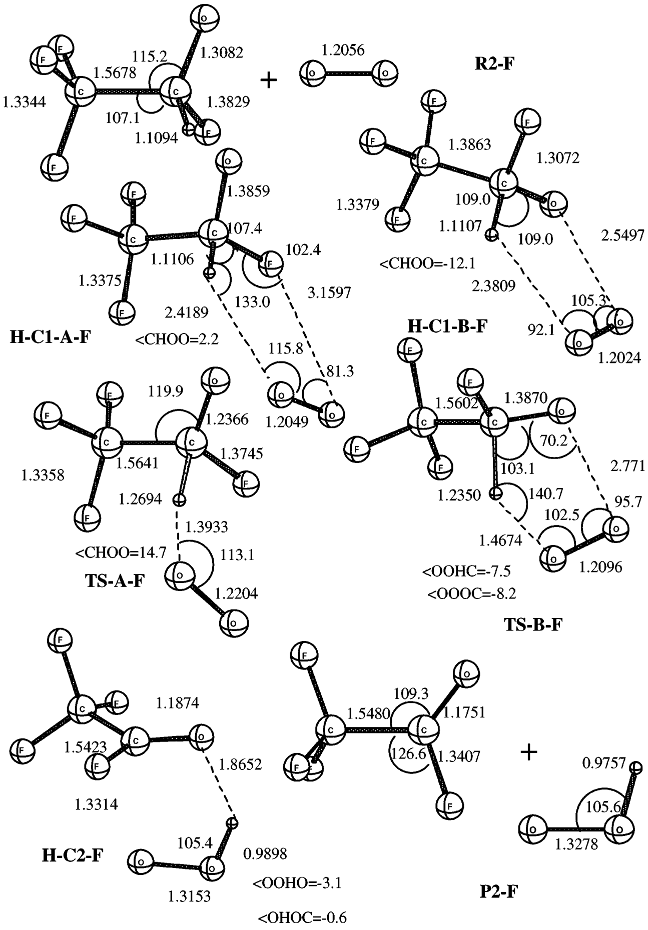

Figure 4. B3LYP/I structures of reactants, transition states, and products for the reaction of CF_3CFHO with O_2. All bond lengths are in angstroms and angles are in degrees.

For reaction 1, an experimental result taken from Bednarek et al.[31] is displayed for comparison to the computed result. Our G2M(CC,MP2) calculations display excellent agreement with this experimental data. For reaction 2, the computed result is compared to experimental data referenced by Bednarek,[31] a computational result of Schneider et al.[9] and additionally to an "experimental" result obtained from recent enthalpy of formation data. Recent experimental enthalpy of formation data[33] are available for a large number of hydrocarbon radicals and some fluorinated species, but data for analogous fluorine compounds are in general sparse and no experimental data are available for CF_3CFHO and CFHO. The enthalpy of reaction 2 is computed by taking a theoretical value for $\Delta H_{f,298}$ (CF_3CFHO) provided by Wu and Carr,[10] a recent computational result[34] of Schneider and Wallington for the enthalpy of formation of CFHO, and experimental data[33] for the enthalpy of formation of CF_3. The G2M(CC,MP2) result for reaction 2 is in poor agreement with the experimental result reported by Bednarek,[31] but does appear to be in better agreement with a computation of ΔE at 0 K by Schneider et al.[9] and the result obtained by combining experimental enthalpy of formation data with computational data. Reactions 3 and 4 are compared to reaction enthalpies computed with experimental enthalpy data.[33] Discrepancies between G2M(CC,MP2) and experiment are between 3 and 5 kcal/mol.

Table 1 also displays more intensive computations of the reaction enthalpy in which base energies for reactions and products have been made using the CCSD(T) method with a cc-PVTZ basis set (basis set III). CCSD(T)/III reaction enthalpies exhibit agreement with experiment that is relatively poor

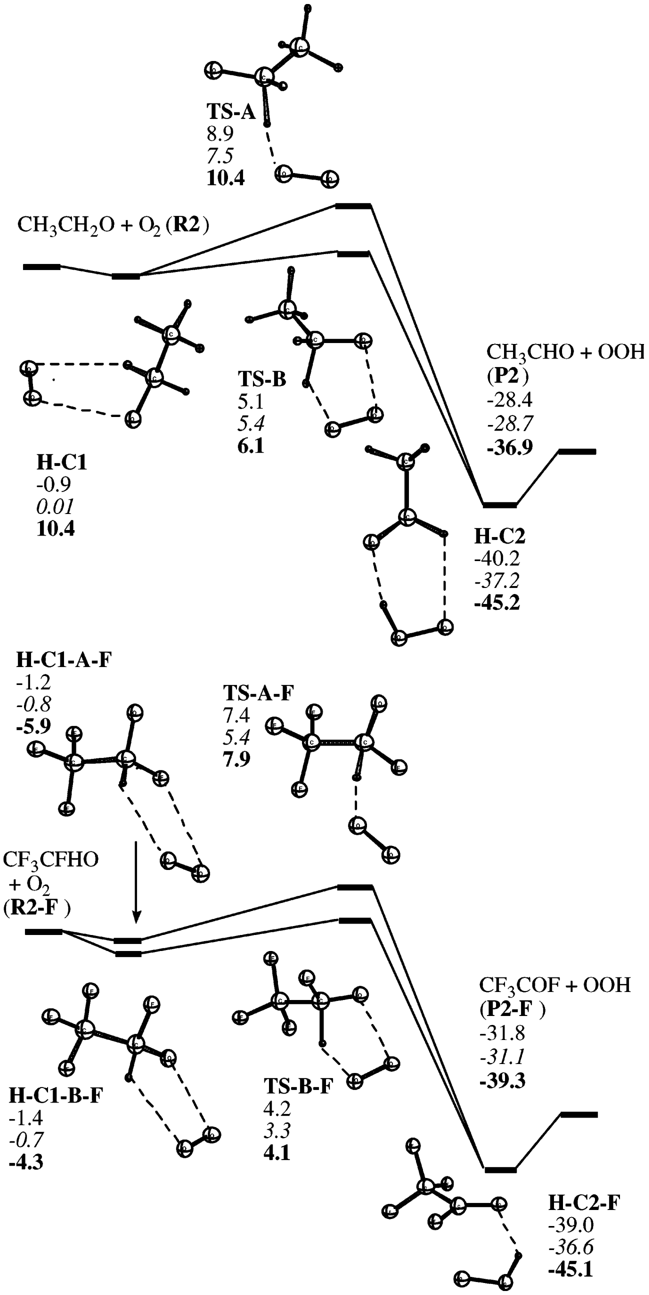

Figure 5. Reaction paths for $CH_3CH_2O + O_2 \rightarrow CH_3CHO + OOH$ and $CF_3CFHO + O_2 \rightarrow CF_3COF + OOH$. B3LYP, B3LYP+ZPE (italic), and G2M(CC,MP2) (bold) energies are displayed. Energies are relative to reactants and are in kcal/mol.

for reactions in which the reactants and products differ in the number of unpaired electrons. The computed CCSD(T)/III energies, unlike G2M(CC,MP2) energies, include no empirical high-level correction (HLC), which serves to make minor adjustments in the energy based on the number of unpaired electrons. No HLC correction has been specifically parametrized for CCSD(T)/III calculations, but an approximate correction has been made by adding the HLC defined for G2M(CC,MP2) to the CCSD(T)/III base energies, with a substantial improvement in agreement with experiment. Such CCSD(T)/III + HLC enthalpies (including B3LYP/I enthalpy correction) are included in Table 1. These enthalpies agree very well with the experimental enthalpy of reaction 1 and with the computational results (b,c) for reaction 2. These computations, like the G2M(CC,MP2) results, show a persistent deviation from experiment of ~3 kcal/mol for reaction 4, but display an error of only 1.6 kcal/mol for reaction 3.

IV. Modeling of Rate Constants

Modeling of the rate constants of reactions 1−4 was attempted with the activated complex (transition state) theory.[16,35,36] For second-order reactions, such as the reaction of an alkoxy radical with O_2, this gives

$$k = (RT/P^0)(k_bT/h)\exp(-\Delta H_a/RT)\exp(\Delta S_a/R)$$

while the rate constant of a first-order unimolecular decomposition is given by

$$k = (k_bT/\mathrm{h})\exp(-\Delta H_a/RT)\exp(\Delta S_a/R)$$

where P^0 is the standard pressure, k_b is the Boltzmann constant, h is Planck's constant, R is the gas constant, T is temperature (taken as 298 K), and ΔH_a and ΔS_a are the changes in standard enthalpy and entropy of activation at 298 K. These last are the difference between the enthalpy (or entropy) of the transition state and reactants. Identifying the activation energy as $\Delta H + RT$ for first-order processes and $\Delta H + 2RT$ for second-order processes provides formulas for the activation energy and gives the relation

$$A = e^2(kT/h)(RT/P^0)\exp(\Delta S_a/R)$$

for second-order processes and

$$A = e(k_bT/h)\exp(\Delta S_a/R)$$

for first-order processes, where e is the exponential constant. The enthalpy of an optimized reactant or transition state is defined in the same manner that enthalpies of reactants and products were defined in section III-D. The entropy of an optimized reactant or transition state is similarly taken as the standard gas-phase entropy at 298 K as determined by Gaussian 98 B3LYP/I frequency computations and subsequent statistical mechanical evaluation.

Table 2 presents rate constants and kinetic parameters (preexponential factors A and activation energies E_a) at 298 K and 1 atm for reactions 1−4 as computed by the methods described above. For comparison, Table 2 also displays rate constants determined at temperatures near 298 K and accompanying kinetic parameters provided in studies referenced in this paper. Particulars of our determinations of the data in this table and data extracted from referenced works are in the following paragraphs.

For CF_3CFHO, our modeled rate constant for reaction with oxygen $k_{O2,F}$ is taken as the sum of the rate constants determined at the two direct abstraction transition states, $k_{O2,F} = k_{O2,F}$(**TS-A-F**) + $k_{O2,F}$(**TS-B-F**). Evaluation of rate constants as described above gives $k_{O2,F}$(**TS-B-F**) = 1.01×10^{-17} cm^3/s and $k_{O2,F}$(**TS-A-F**) = 1.16×10^{-19} cm^3/s for a total $k_{O2,F}$ of 1.02×10^{-17} cm^3/s. This value is smaller than all previous estimates of k_1. For example, this is 2 orders of magnitude smaller than Bednarek's[5] direct experimental determination of $k_1 = 2.7 \times 10^{-15}$ cm^3/s. Somnitz and Zellner[10] and Wu and Carr[8] estimate k_1 from combinations of experimental data and ab initio/RRKM models and also obtain values of k_1 larger than ours. The rate constant $k_{O2,F}$(**TS-B-F**) by far makes the most significant contribution to $k_{O2,F}$; the modeled A factor for this rate constant is $A_{O2,F} = 3.06 \times 10^{-14}$ cm^3/s; the associated activation energy is $E_{a,O2,F} = 4.7$ kcal/mol.

TABLE 1: B3LYP/I, G2M(CC,MP2), CCSD(T)/III, and Experimental Enthalpies (298 K, kcal/mol) of Various Reactions

reaction	B3LYP/I	G2M(CC,MP2)	CCSD(T)/III	CCSD(T)/III + HLC	expt.
1. $CF_3CFHO + O_2 \rightarrow CF_3COF + OOH$	−31.6	−37.0	−34.5	−37.8	−38.0[a]
2. $CF_3CFHO \rightarrow CF_3 + CFHO$	0.9	2.2	2.0	2.0	8.1,[a] 0.3,[b] 0.3[c]
3. $CH_3CH_2O + O_2 \rightarrow OOH + CH_3CHO$	−28.2	−37.4	−31.1	−34.3	−32.7[d]
4. $CH_3CH_2O \rightarrow CH_2O + CH_3$	13.4	10.1	10.5	10.5	12.8[d]

[a] Reference 31. [b] Reference 9, computational result. (ΔE for the reaction at 0 K is computed by approximation to CCSD(T)/TZ2P calculations at MP2/6-31G(d,p) geometries.) [c] Enthalpies of formation are taken from refs 33 (CF_3), 34 (CFHO, computational result, approximation to QCISD(T)/aug-cc-pVTZ calculations at MP2/6-31G(d,p) geometries), and 8 (CF_3CFHO, computational result, G2MP2). [d] Enthalpies of formation are taken from ref 33.

TABLE 2: Rate Constants and Arrhenius Parameters (*A* and E_a) of Reactions 1−4 at Temperatures Near 298 K (Pressures for Pressure-Dependent Rate Constants (Reactions 2 and 4) Are 1 atm Unless Otherwise Noted)

reaction	*k*	*A*	E_a	ref
1	2.7×10^{-15} cm^3/s (295 K)			5,12
	4.75×10^{-15}−1.9×10^{-14} cm^3/s (295 K)	7.5×10^{-15}−4.8×10^{-13} cm^3/s[a]	−0.5 to 1.9 kcal/mol[a]	8
	4.2×10^{-16} cm^3/s (300 K)	3.06×10^{-14} cm^3/s	4.7 kcal/mol	10
	1.02×10^{-17} cm^3/s (298 K)			this work
2	9.8×10^{4} s^{-1} (298 K)	7.4×10^{11} s^{-1}	9.4 kcal/mol	2
	1.8×10^{4} s^{-1}[b] (295 K, 50 mbar)			5
	4.56×10^{4} s^{-1} (297 K)		9.5 kcal/mol[c]	8
	2.1×10^{5} s^{-1} (298 K)	4.8×10^{13} s^{-1}	11.4 kcal/mol	9
	1.1×10^{4} s^{-1} (300 K, 1 bar)	9.58×10^{12} s^{-1}	12.2 kcal/mol	10
	1.33×10^{5} s^{-1} (298 K)	1.06×10^{14} s^{-1}	12.1 kcal/mol	this work
3	1.0×10^{-14} cm^3/s (298 K)	7.1×10^{-14} cm^3/s[d]	1.10 kcal/mol[d]	14,15
	1.4×10^{-14} cm^3/s (298 K)	3.0×10^{-13} cm^3/s	1.84 kcal/mol	18
	7.8×10^{-15} cm^3/s (296 K)			19
	2.52×10^{-19} cm^3/s (298 K)	7.9×10^{-15} cm^3/s	6.1 kcal/mol	this work
4	0.144 s^{-1} (298 K)	1.0×10^{15} s^{-1}	21.6 kcal/mol	20,21
	5.31 s^{-1} (298 K)[e]	1.1×10^{13} s^{-1}	16.8 kcal/mol	22
	6.2×10^{-3} s^{-1} (298 K)[f]	7.9×10^{13} s^{-1}	22.0 kcal/mol	23
	1.46 s^{-1} (300 K, 1bar)	9.8×10^{12} s^{-1}	17.6 kcal/mol	24
	7.03 s^{-1} (298 K)	2.4×10^{13} s^{-1}	17.1 kcal/mol	this work

[a] Applies to estimate of $k_1 = 1.9 \times 10^{-14}$ cm^3/s. [b] Should be multiplied by approximately 1 order of magnitude to obtain *k* at 1 atm, as noted in text. [c] G2 barrier height. [d] Reference 14. [e] High (infinite)-pressure limit. [f] High-pressure limit.

The rate for C−C scission breaking in CF_3CFHO is calculated for one reaction pathway taking **TS-CC-F** as the transition state. This gives a modeled rate constant $k_{CC,F} = 1.33 \times 10^5$ s^{-1}, a result within an order of magnitude or less than other studies displayed. This is an order of magnitude smaller than Bednarek's[5] recent experimental value (at 295 K and 38 Torr) of $k_2 = 1.8 \times 10^4$ s^{-1}. The pressure-dependence studies of Wallington et al.[6] indicate that Bednarek's result would be multiplied by approximately an order of magnitude in the high-pressure limit. Our results are similar to those of several recent[8−10] computational studies, particularly the ab initio/RRKM results of Somnitz and Zellner.[10] Our modeling obtains an *A* factor $A_{CC,F} = 1.06 \times 10^{14}$ s^{-1}, with associated activation energy activation energy $E_{a,CC,F} = 12.1$ kcal/mol. These values may be compared to the value of $A = 4.8 \times 10^{13}$ s^{-1} and $E_a = 11.4$ kcal/mol Schneider obtained[9] using ab initio calculations combined with canonical transition state theory. Somnitz and Zellner's computations[10] obtain an *A* factor of 9.58×10^{12} s^{-1} and activation energy $E_a = 12.2$ kcal/mol at a pressure of 1 bar. The rate constant ratio is $k_{o2,F}/k_{CC,F} = 7.69 \times 10^{-23}$ cm^3, 3 orders of magnitude smaller than Wallington's[7] value of 4.0×10^{-20} cm^3, as noted in the Introduction. The discrepancy may arise from our evaluation of k_1, as noted above.

For CH_3CH_2O, we again take the rate of reaction with O_2 (reaction 3) as the sum of rate constants corresponding to transition states **TS-A** and **TS-B** or $k_{O2} = k_{O2}$(**TS-A**) + k_{O2} (**TS-B**). Evaluation of rate constants gives k_{O2}(**TS-B**) = 2.49×10^{-19} cm^3/s, k_{O2} (**TS-A**) = 2.35×10^{-21} cm^3/s, and $k_{O2} = 2.52 \times 10^{-19}$ cm^3/s, a value which is again orders of magnitude smaller than previous experimental determinations,[14,15,18,19] as shown in Table 2. The *A* factor for k_{O2}(**TS-B**) is A_{O2}(**TS-B**) = 7.9×10^{-15} cm^3/s, with accompanying activation energy E_a(**TS-B**) = 6.1 kcal/mol. This *A* factor is lower by an order of magnitude than the most recent experimental value[14] of 7.1×10^{-14} cm^3/s. The activation energy is several kcal/mol higher than indicated in previous experimental determinations.[14,18] This suggests that the computed energy barrier posed by **TS-B** may be too high. More computationally rigorous determinations of the energy of **TS-B** are described later in this section.

The modeled rate constant for C−C breaking, k_{CC}, is found for one path with **TS-CC** as the transition state; evaluation gives $k_{CC} = 7.03$ s^{-1}. Earlier experimental results[20,21] give a value of $k_4 = 0.144$ s^{-1} at 298 K and pressures near 1 atm, which studies[21,22] indicate is near the high-pressure limit for alkoxy radicals. More recent experimental studies[22] obtain the expression $k_4 = 1.1 \times 10^{13} \exp(-70.3\ \text{kJ/mol}/RT)$ in the high-pressure limit, which gives a value of 5.31 s^{-1}. This experimental expression for k_4 is in close agreement with ab initio/RRKM studies in the same work.[22] The ab initio/RRKM study of Hoyermann et al.[23] yields Arrhenius parameters (in the high-pressure limit) of $A = 7.9 \times 10^{13}$ s^{-1} and $E_a = 22.0$ kcal/mol; at 298 K this gives a rather low value of $k_4 = 6.2 \times 10^{-3}$ s^{-1}. Our *A* factor for k_{CC} is $A_{CC} = 2.4 \times 10^{13}$ s^{-1}, with accompanying activation energy $E_{a,CC} = 17.1$ kcal/mol; the *A* factor is 2 orders of magnitude beneath the earlier experimental value of 1.0×10^{15} s^{-1},[20,21] but comparable to the more recent value of 1.1×10^{13} s^{-1} noted above.[22]

This modeling lends support to the contention that the reaction of CF_3CFHO with O_2 is more rapid than its unfluorinated analogue ($k = 1.02 \times 10^{-17}$ cm^3/s for CF_3CFHO vs $k = 1.59 \times 10^{-21}$ cm^3/s). The rate of reaction of the fluorinated compound is 4 orders of magnitude larger than that for the unfluorinated compound, a result greater than the 2 orders of magnitude difference suggested by Wallington et al.[6] The larger rate constant is a result primarily of the smaller barrier to reaction for CF_3CFHO (4.1 kcal/mol for **TS-B-F** vs 6.1 kcal/mol for **TS-B**, considering the barrier posed by the more stable transition state as provided by standard G2M(CC,MP2) calculations). This result is naturally subject to errors in the computed energies of the transition state. Section III-E compares the enthalpies of computed G2M(CC,MP2) reactions and experiment; the largest discrepancy occurs in reaction 3. The G2M(CC,MP2) energy of **TS-B**, which lies on the path of reaction 3, may be particularly inaccurate.

The CCSD(T)/III + HLC reaction enthalpies shown in Table 1 display excellent agreement with experiment for both reactions 1 and 3. A comparison of the CCSD(T)/III + HLC relative energies of **TS-B** and **TS-B-F** might provide a more reliable estimate of relative barrier heights than a comparison of G2M(CC,MP2) results. However, the expense of a CCSD(T)/III calculation of **TS-B-F** prohibited this computation. A CCSD(T)/III + HLC calculation of the energy of **TS-B** relative to the reactants was feasible. This calculation determined a barrier height of 6.2 kcal/mol; this result incorporates B3LYP/I zero-point energy corrections for better comparison to the G2M(CC,MP2) results, which also incorporate this ZPE correction.

The G2M(CC,MP2) enthalpy of reaction 1 and the CCSD(T)/III +HLC energy of reaction 3 both show close (less than 2 kcal/mol) agreement with experiment, suggesting that the G2M(CC,MP2) energy of **TS-B-F** and the CCSD(T)/III + HLC energy of **TS-B** may provide energies close to the true barrier heights of reactions 1 and 3, and it is worthwhile to compare the two. The high-level CCSD(T)/III + HLC calculation of **TS-B** finds a barrier height of 6.2 kcal/mol; this number is approximately 2 kcal/mol higher than the G2M(CC,MP2) relative energy of **TS-B-F**. As the CCSD(T)/III + HLC relative energy of **TS-B** is essentially the same as the relative energy at the G2M(CC,MP2) level, substitution of the CCSD(T)/III + HLC energy into the computation of k_{O2} discussed above makes little difference in the results.

V. Summary

The final paragraph of the Introduction of this paper poses three significant questions, and the results supplied in the subsequent sections provide indications of the possible answers. To address the first question, the computations presented here do suggest that CF_3CFHO reacts more rapidly with O_2 than its unfluorinated analogue, CH_3CH_2O. It may be true that fluorinated alkoxy radicals in general react more rapidly with O_2 than unfluorinated ones. Future computational and experimental studies on other systems may make it possible to directly compare rate constants for fluorinated alkoxy radicals with their unfluorinated analogues and provide more insight into this question.

To speak to the second question, this study finds no substantial differences between the reaction mechanisms of reactions 1 and 3. The results indicate that the reaction of CF_3CFHO with O_2 occurs by means of transition states very similar to those of the reaction of CH_3CH_2O with O_2. The calculations suggest that reaction occurs more rapidly for the fluorinated compound primarily because the energetic barrier to reaction posed by the transition state is lower than that for the unfluorinated analogue. Our best computations indicate that the barrier to reaction is approximately 2 kcal/mol higher in the unfluorinated species. This suggests the possibility that fluorinated alkoxy radicals in general have lower barriers to reaction with O_2 than their unfluorinated analogues. Further computational work comparing fluorinated and unfluorinated systems might lend additional support to this hypothesis.

Concerning the third question, our ratio of *A* factors for fluorinated and unfluorinated compounds is nearly equal. The ratio of *A* factors $A_{O2,F}/A_{CC,F} = 2.89 \times 10^{-28}$; this is 3 orders of magnitude smaller than Wallington's value of 2.1×10^{-25}.[9] The computed ratio of *A* factors for the reactions of CH_3CH_2O is $A_{O2}/A_{CC} = 3.24 \times 10^{-28}$ cm^3. This *A* factor ratio should be compared to the ratio of *A* factors obtained by taking the *A* factor for reaction with O_2 reported by Hartmann,[14] and dividing by Caralp's[22] experimental *A* factor for decomposition; this gives a value of (7.1×10^{-14} cm^3/s/1.1×10^{13} s^{-1}) = 6.4×10^{-27} cm^3 for A_3/A_4. The modeling deviates from experiment by an order of magnitude. These results do not support earlier speculations that the *A* factor ratio will be much larger for CF_3CFHO. We note that the modeled *A* factor for the reaction of CF_3CFHO with O_2, $A_{O2,F} = 3.06 \times 10^{-14}$, is larger than the corresponding *A* factor for CH_3CH_2O, $A_{O2} = 7.9 \times 10^{-15}$. This difference of an order of magnitude is in qualitative agreement with the hypothesis of Schneider et al.[9] However, the decomposition rate constants also differ by an order of magnitude; the modeled decomposition *A* factor for CF_3CFHO, $A_{CC,F} = 1.06 \times 10^{14}$ s^{-1}, is an order of magnitude larger than the modeled *A* factor for the unfluorinated analogue, $A_{CC} = 2.4 \times 10^{13}$.

Acknowledgment. We acknowledge William L. Hase for private discussions of modeling rate constants. We also thank Keiji Morokuma for valuable advice. The Cherry L. Emerson Center of Scientific Computation at Emory University granted a fellowship to J.E.S. that provided facilities for this research. This research was also supported by the National Center for Supercomputing Applications (Grant No. CHE010014N) and the Petroleum Research Fund (Grant No. 37058-GB6).

References and Notes

(1) Wallington, T. J.; Schneider, W. F.; Sehested, J.; Nielsen, O. J. *J. Chem. Soc., Faraday Discuss.* **1996**, *100*, 55.

(2) Rattigan, O. V.; Rowley, D. M.; Wild, O.; Jones, R. L. *J. Chem. Soc., Faraday Trans.* **1994**, *90*, 1819−1829.

(3) Wallington, T. J.; Hurley, M. D.; Ball, J. C.; Kaiser, E. W. *Environ. Sci. Technol.* **1992**, *26*, 1318−1324.

(4) Tuazon, E. C.; Atkinson, R. *J. Atmos. Chem*. **1993**, *16*, 301.

(5) Bednarek, G.; Breil, M.; Hoffman, A.; Kohlmann, J. P.; Mors, V.; Zellner, R. *Ber. Bunsen-Ges. Phys. Chem*. **1996**, *100*, 528−539.

(6) Wallington, T. J.; Hurley, M. D.; Frachboud, J. M.; Orlando, J. J.; Schested, J.; Mogelberg, T. E.; Nielsen, O. J. *J. Phys. Chem.* **1996**, *100*, 18116−18122.

(7) Wallington, T. J.; Kaiser, E. W. *Int. J. Chem. Kinet.* **1999**, *31*, 397−398.

(8) Wu, F.; Carr, R. W. *J. Phys. Chem. A* **2003**, *107*, 10733−10742.

(9) Schneider, W. F.; Wallington, T. J.; Barker, J. R.; Stahlberg, E. A. *Ber. Bunsen-Ges. Phys. Chem*. **1998**, *102*, 1850−1856.

(10) Somnitz, H.; Zellner, R. *Phys. Chem. Chem. Phys*. **2001**, *3*, 2352−2364.

(11) Tromp, T. K.; Ko, M. K. W.; Rodriguez, J. M.; Sze, N. D. *Nature* **1995**, *376*, 327.

(12) Data taken from ref 2, which attributes: Zellner, R.; Hoffmann, A.; Bingemann, D.; Mors, V.; Kohlman, P. J. P. "Kinetics and Mechanisms for the Reactions of Halogenated Organic Compounds in the Troposhere"; STEP-HALOCSIDE/AFEAS Workshop, Dublin, 1991.

(13) Wu, F.; Carr, R. W. *J. Phys. Chem.* **1996**, *100*, 9352−9359.

(14) Hartmann, D.; Karthauser, J.; Sawerysyn, J. P.; Zellner, R. *Ber. Bunsen-Ges. Phys. Chem*. **1990**, *94*, 639−645.

(15) Taken from ref 6, which cites: Demore, W. B.; Sander, S. P.; Golden, D. M.; Hampson, R. F.; Kurlyo, M. J.; Howard, C. J.; Ravishankara, A. R.; Kolb, C. E.; Molina, M. J. JPL Publication 94-26, 1994.

(16) Benson, S. W. *Thermochemical Kinetics*; Wiley: New York, 1976.

(17) Taken from ref 9, which cites: Atkinson, R.; Baulch, D. L.; Cox, R. A.; Hampson, J. F., Jr.; Kerr, J. A.; Troe, J. *J. Phys. Chem. Ref. Data* **1992**, *21*, 1125.

(18) Zabarnick, S.; Heicklen, J. *Int. J. Chem. Kinet.* **1985**, *17*, 455−476.

(19) Gutman, D.; Sanders, N.; Butler, J. E. *J. Phys. Chem.* **1982**, *86*, 66−70.

(20) Batt, L. *Int. J. Chem. Kinet*. **1979**, *11*, 977−993.

(21) Batt, L.; Milne, R. T. *Int. J. Chem. Kinet.* **1977**, *9*, 549−565.

(22) Caralp, F.; Devolder, P.; Fittschen, C.; Gomez, N.; Hippler, H.; Mereau, R.; Rayez, M. T.; Striebel, F.; Viskolcz, B. *Phys. Chem. Chem. Phys*. **1999**, *13*, 2935−2944.

(23) Hoyermann, K.; Olzmann, M.; Seeba, J.; Viskolcz, B. *J. Phys. Chem. A* **1999**, *103*, 5692−5698.

(24) Somnitz, H.; Zellner, R. *Phys. Chem. Chem. Phys*. **2000**, *2*, 1899−1905. Somnitz, H.; Zellner, R. *Phys. Chem. Chem. Phys*. **2000**, *2*, 1907−1918. Somnitz, H.; Zellner, R. *Phys. Chem. Chem. Phys*. **2000**, *2*, 4319−4325.

(25) Gonzales, C.; Sosa, C.; Schlegel, H. B. *J. Phys. Chem.* **1989**, *93*, 2435−2440.

(26) Jungkamp, T. P. W.; Seinfeld, J. H. *Chem. Phys. Lett*. **1996**, *263*, 371−378.

(27) Bofill, J. M.: Olivella, S.; Sole, A.; Anglada, J. M. *J. Am. Chem. Soc*. **1999**, *121*, 1337−1347.

(28) Frisch, M. J.; Trucks, G. W.; Schlegel, H. B.; Scuseria, G. E.; Robb, M. A.; Cheeseman, J. R.; Zakrzewski, V. G.; Montgomery, J. A., Jr.; Stratmann, R. E.; Burant, J. C.; Dapprich, S.; Millam, J. M.; Daniels, A. D.; Kudin, K. N.; Strain, M. C.; Farkas, O.; Tomasi, J.; Barone V.; Cossi, M.; Cammi, R.; Mennuci, C.; Pomelli, C.; Adamo, C.; Clifford, S.; Ochterski, J.; Petersson, G. A.; Ayala, P. Y.; Cui, Q.; Morokuma, K.; Malick, D. K.; Rabuck, A. D.; Ragivachari, K.; Foresman, J. B.; Ciolowski, J.; Ortiz, J. V.; Stefanov, B. B.; Liu, G.; Liashenko, A.; Piskorz, P.; Komaromi, I.; Gomperts, R.; Martin, R. L.; Fox, D. J.; Keith, T.; Al-Laham, M. A.; Peng, C. Y.; Nanayakkara, A.; Gonzales, C.; Challacombe, M.; Gill, P. M. W.; Johnson, B.; Chen, W.; Wong, M. W.; Andres, J. L.; Gonzales, C.; Head-Gordon, M.; Replogle, E. S.; Pople, J. A. Gaussian 98, revision A.1; Gaussian, Inc.: Pittsburgh, PA, 1998.

(29) Becke, A. D. *J. Chem. Phys*. **1992**, *96*, 2155−2160. Becke, A. D. *J. Chem. Phys*. **1993**, *98*, 5648−5652.

(30) Mebel, A. M.; Morokuma, K.; Lin, M. C. *J. Chem. Phys.* **1995**, *103*, 7414−7421.

(31) Data taken from ref 5, which cites: Zellner, R. Scientific Assessment of Stratospheric Ozone, WMO Report 20, Vol. II, Appendix AFEAS Report, 251, 1989.

(32) See, for example: McQuarrie, D. *Statistical Mechanics*; Harper and Row: New York, 1976.

(33) Enthalpies of formation are taken from: Sander, S. P.; Friedl, R. R.; Ravishankara, A. R.; Golden, D. M.; Kolb, C. E.; Kurylo, M. J.; Huie, R. E.; Orkin, V. L.; Molina, M. J. “Chemical Kinetics and Photochemical Data for Use in Stratospheric Modeling”, Evaluation Number 14, NASA JPL Publication 2003; No. 02-25.

(34) Schneider, W. F.; Wallington, T. J. *J. Phys. Chem.* **1994**, *98*, 7448−7451.

(35) Atkins, P. *Physical Chemistry*, 6th ed.; W. H. Freeman and Co.: New York, 1998.

(36) Gardiner, W. C., Jr. *Rates and Mechanisms of Chemical Reactions*; W. A. Benjamin: New York, 1969.